1990SvAL...16..160A

with typical scale 400-500 km across the orbit of Phobos was observed in the TAUS data on the first and third elliptical orbits (on the second elliptical orbit, the expected decrease coincided with the periodic decrease in the ion flux due to the rotation of the spacecraft). It should be noted that during these crossings of the orbit of Phobos by the spacecraft, the Martian moon itself was located far from it. In this case, to explain the observed events it is necessary to assume the presence in the orbit of Phobos of a belt of gas, dust, or larger particles. Previously, this idea was discussed by Ip (1988) and Soter (1971). However, this interpretation should not be considered as definitive, since similar disturbances of the solar wind flux were observed by the TAUS experiment in other parts of the orbit as well.

Dolginov, Sh. Sh., Eroshenko, E. G., Zhuzgov, L. N., et al. (1976). Solar Wind Interaction with the Planets Mercury, Venus, and Mars (ed. N.F. Ness), NASA SP-397, p. 1.

Eastman, T. E., DeCoster, R. J., and Frank, L. A. (1986). Ion Acceleration in the Magnetosphere and Ionosphere (ed. T. Change), Amer. Geophys. Union, Washington, D.C., p. 433.

Gringauz, K. I. (1976). Rev. Geophys. and Space Phys. 14, 391.

Gringauz, K. I. (1981). Adv. Space Res. 1, 5.

Gringauz, K. I., Bezrukikh, V. V., Verigin, M. I., and Remizov, A. P. (1976). J. Geophys. Res. 81, 3349.

Ip, W.-H. (1988). Icarus 76, 135.

Kennel, C. F. (1989). Personal communication.

Krasnopol'skii, V. A. (1982). Photochemistry of the Atmospheres of Mars and Venus [in Russian], Nauka, Moscow.

Nagy, A. F. and Cravens, T. E. (1988). Geophys. Res. Lett. 15, 433.

Rosenbauer, H., Shutte, N., apathy, I. et al. (1989). Instrumentation and Methods for Scientific Space Studies [in Russian] (ed. V. M. Balebanov), Nauka, Moscow, p. 3.

Shutte, N. M., Kiraly, P., Cravens, T., et al. (1990). Pis'ma Astron. Zh. 16, 363 [Sov. Astron. Lett. 16, 154 (1990)].

Soter, S. (1971). "The dust belt of Mars," Preprint of Center for Radiophysics and Space Research, Cornell University, CRSR-462.

Translated by P. J. Moxhay

Television pictures of Phobos: first results

G. A. Avanesov, B. I. Bonev, F. Kempe, A. T. Bazilevskii, V. Boicheva, G.-G. Wiede, P. Gromatikov, T. Duxbury, M. Danz, D. Dimitrov, B. S. Zhukov, Ya. L. Ziman, V. Kolev, V. I. Kostenko, V. A. Kottsov, V. M. Krasavtsev, V. A. Krasikov, A. Krumov, A. A. Kuz'min, K. D. Losev, K. Lumme, D. Mohlmmann, S. Murchie, D. N. Mishev, K. Muinonen, V. M. Murav'ev, B. Murray, W. Neumann, L. Paul, W. Possel, D. Petkov, P. Petukhova, B. Rebel, S. Simeonov, B. Smith, A. Totev, Yu. Uzunov, V. P. Fedotov, D. Halman, J. Head, V. N. Heifets, H. Zapfe, K. N. Chikov, and Yu. G. Shkuratov

Space Research Institute, USSR Academy of Sciences, Moscow;
Institute for Precision Mechanics and Optics, Leningrad;
Space Research Institute, Bulgarian Academy of Sciences, Sofia;
Institute for Cybernetics and Information Processes, East German Academy of Sciences, Berlin;
Space Research Institute, East German Academy of Sciences, Berlin;
Institute of Geochemistry and Analytical Chemistry, USSR Academy of Sciences, Moscow;
Kharkov University;
Brown University, Providence;
Jet Propulsion Laboratory, Pasadena;
Helsinki University;
California Institute of Technology, Pasadena;
and University of Arizona, Tucson

(Submitted September 4, 1989)

Pis'ma Astron. Zh. **16**, 378–388 (April 1990)

In February-March 1989, 37 television images of the Martian satellite Phobos were obtained by the Phobos 2 spacecraft from distances of 200–1100 km. These images provide an important supplement to the TV data from the American Mariner 9 and Viking spacecraft in coverage of the surface of Phobos and in resolution in certain regions, in spectral range, and in range of phase angles. They make it possible to refine the figure and topographic and geological maps of the surface of Phobos, its spectral and angular reflective characteristics, the surface composition and texture, and characteristics of the orbital and librational motion.

PREPARATION AND EXECUTION OF THE EXPERIMENT

The primary tasks of the TV experiment were: a) photography of Phobos from circular and quasi-synchronous orbits for global studies of its surface, as well as to refine its orbital motion with the aim of the real-time solution of the navigation of problems; b) photography of Phobos with centimeter resolution during the planned drift of the automatic interplanetary station (AIS) at an altitude of 50 m above the surface of Phobos.

To solve these problems, specialists from Bulgaria, East Germany, and the USSR have developed the Fregat videospectrometric complex (VSC), which incorporates a three-channel TV camera, a spectrometer, and a 1.5 Gbit video recorder (a limited amount of video data could also be stored in the

 © 1990 American Institute of Physics

© American Institute of Physics • Provided by the NASA Astrophysics Data System

1990SvAL...16..160A

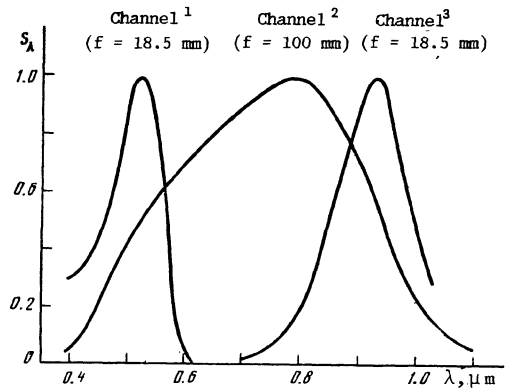

FIG. 1. Spectral sensitivity of the VSC TV channels.

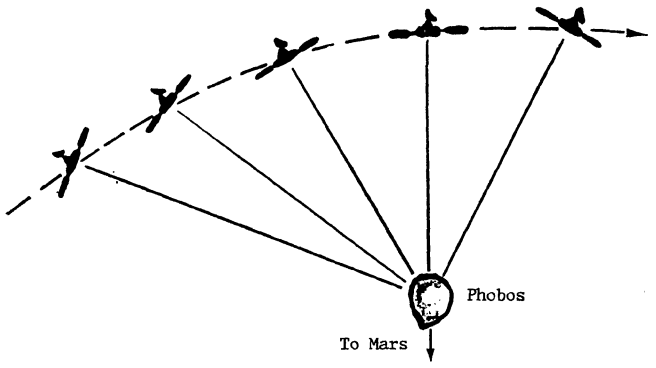

FIG. 2. Scheme of TV photography of Phobos.

main memory of the Morion scientific instrument complex). The TV camera had two short-focus (f = 18.5 mm) channels and one long-focus (f = 100 mm) channel with angular resolutions of 3.3 × 4.5 and 0.62 × 0.83 arcmin, respectively. The spectral sensitivity of the TV channels is shown in Fig. 1. For the radiation receivers in the TV camera and the spectrometer, CCD arrays were used, which had two sections — storage and memory — with a working size of 288 × 505 elements (the "electron gate" principle was used in the VSC).

Unfortunately, because of the premature loss of the Phobos AISs, the TV investigations were confined to photographs from circular and quasi-synchronous orbits, from distances of 200-1100 km. The scheme of the Phobos photography is shown in Fig. 2. The photographs were made in series of three images each (one image in each channel), recording the video data in the Morion. The time interval between images was 1 min 20 sec and that between series was 15-30 min. Before the start of each series, the AIS was aimed at Phobos, and its orientation remained constant during the series. The photography run on 21 February 1989 consisted of three series and those on 28 February and 25 March 1989 consisted of five series. We obtained a total of 37 images of Phobos, as well as Phobos against the background of Mars. Examples of these images are given in Fig. 3.

DISCUSSION

The images that were obtained show most of the surface of Phobos except for the vicninity of the sub-Martian point. The least-mapped region, between the crater Stickney and the anti-Martian point (this region was photographed by Viking at oblique observing angles and with a resolution of hundreds of meters), was photographed in the greatest detail, with a resolution down to 40 m/pixel. The new images permit more detailed mapping of the distribution of craters and grooves to the west of Stickney, but now it can be stated that in this region the concentration of grooves is considerably lower than in the region to the east of Stickney, and this is not related to the lower image resolution, as might have been thought earlier.

The location of the control points on the surface of Phobos, for which the centers of large craters were used, agrees well with the data of Duxbury and Callahan (1989), but significant disagreements with Turner's topographic maps (1978) are revealed.

The TV images of Phobos were obtained over a wide range of phase angles, from 7° to 90°. The complex surface relief of Phobos, saturated with craters, is emphasized in images at large phase angles. Crater chains are clearly visible in the central pat of Fig. 3a. The brightness of the images obtained at small phase angles is fairly insensitive to surface slope and is determined mainly by the optical characterisdtics of the surface and its texture. At phase angles of 7°-8° (Fig. 3e), bright rings or arcs, the albedo of which exceeds by 20-30% the mean albedo of the surface of Phobos, are observed on the embankments of many craters. This feature was also noted in Viking images (Thomas, 1978, 1979). At moderate phase angles, the brightness of these sections is comparable with the brightness of the remaining surface: this means that bright albedo formations also have a higher phase coefficient.

TABLE I. Extent of Bright Albedo Formations as a Function of Crater Type

Crater type	Number of craters	Fraction of craters (%) for which albedo formations		
		occupy over half the embankment	occupy less than half the embankment	are absent
Fresh	3	100	–	–
Partly degraded	28	57	15	28
Completely degraded	8	12	38	50
Ghost craters	6	–	33	67

© American Institute of Physics • Provided by the NASA Astrophysics Data System

1990SvAL...16..160A

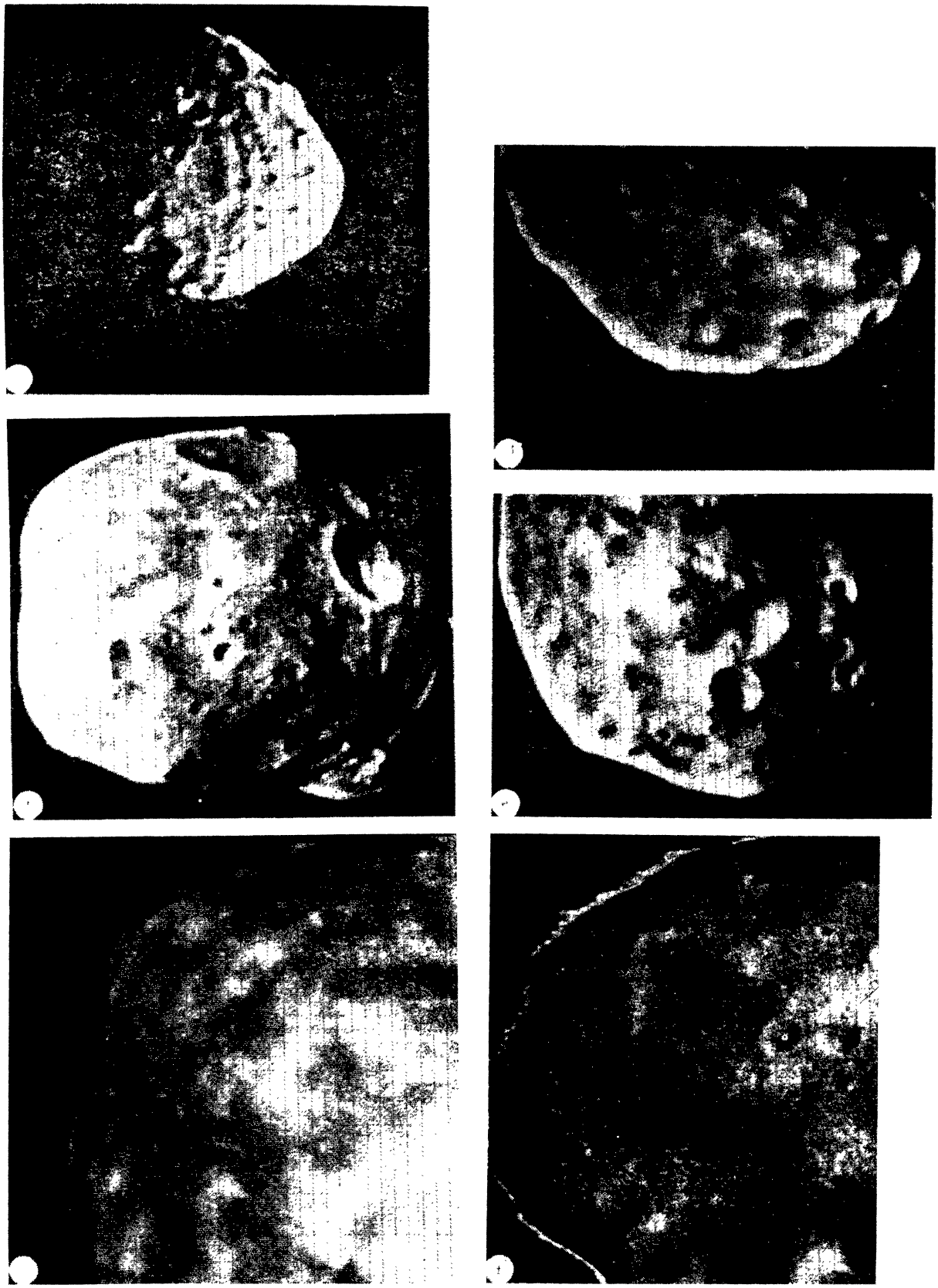

FIG. 3. Processed images of Phobos obtained with the VSC (the processing was done at the Space Research Institute, USSR Academy of Sciences). The channel number, the distance between the AIS and Phobos (km), the size of a pixel (m), and the phase angle (deg) are given for each image: a) 2, 958, 173, 74; b) 2, 439, 79, 24; c) 2, 359, 65, 19; d) 2, 341, 61, 26; e) 2, 302, 37, 7; f) 2, 191, 34, 18; g) 3, 335, 326, 25; h) 1, 192, 187, 19.

© American Institute of Physics • Provided by the NASA Astrophysics Data System

1990SvAL...16..160A

FIG. 3 (continued)

The relation between the extent of albedo formations on crater embankments and their degree of degradation was analyzed on the basis of Phobos 2 and Viking images obtained at small phase angles. We selected 45 craters with a diameter of over 1 km, located between latitude 50° S and 50-70° N, and between longitude 40 and 300° W. The Thomas (1978) scheme of crater classification was used, but the specific typing of the craters was reconsidered with allowance for the new Phobos 2 images. A crater was assigned to one of three groups as a function of the extent of albedo formations: craters for which bright albedo formations are lacking; craters for which they occupy less than half the embankment; and craters for which they occupy over half of the embankment. The results, presented in Table I, convincingly show that bright albedo formations around craters disappear as the craters degrade.

The simultaneous increase in albedo and phase coefficient on the embankment of fresh craters may be related to a difference in both the texture and composition of the reflecting surface layer. Up to now, this effect has been interpreted by assuming that "unusually complex textures" exists on crater embankments, resulting in a strong shadow effect (Veverka, 1978). It must be noted that on such dark bodies as Phobos, the increase in the single-scattering albedo of regolith particles, (Shkuratov, 1988) can be added to this effect in the context of the interference mechanism for producing the opposition effect. The higher albedo of particles on the embankments of fresh craters may be related to the shorter time of its processing by cosmogenic factors (micrometeoritic bombardment, solar wind) due to their more recent formation or due to the uncovering of fresher material under the action of down-slope processes. Under the low-gravity conditions on Phobos, down-slow motion of material may be initiated by seismic vibrations in the body of Phobos during mateorite impacts, as well as by diurnal changes in surface temperature.

The images from Phobos 2 show that the banks of grooves also have an increased brightness at small phase angles (Fig. 3e). An investigation of this phenomenon is of great interest for choosing among existing models of the origin of the grooves on Phobos (Thomas, 1978; Thomas et al., 1979; Head and Cintela, 1979; Wilson and Head, 1989; Head, 1986): a model in which the formation of grooves is associated with impact or tidal fractures in the body of Phobos with a release of volatile components (Thomas, 1978; Thomas et al., 1979); a model that considers grooves to be merged chains of secondary craters (Head and Cintala, 1979); and model according to which grooves were formed in the movement of large fragments of crater ejecta over the surface (Wilson and Head, 1989); these models are consistent with variations of composition and surface texture along the grooves. The model of spreading fissures that fill in which regolith (Thomas et al., 1979) can be reconciled with the presence of lighter material on the banks only by assuming that it is less mature (as in the case of craters).

The photographs, taken over a wide range of phase angles, enable us to supplement ground-based (Zellner and Capen, 1974) and space investigations (Noland and Veverka, 1976; Pang et al., 1983) of the photometric characteritics of the surface of Phobos in the visible and compare them with the first photo-

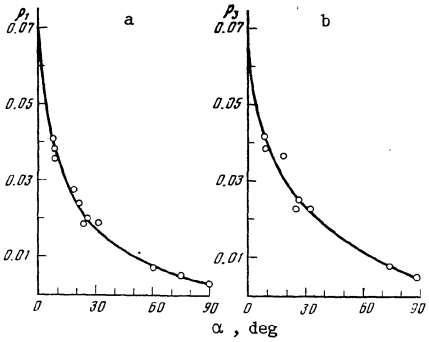

FIG. 4. Brightness factor (ρ) averaged over the disk of Phobos as a function of phase angle (ω) in the visible (channel 1: a) and near- IR (channel 3: b). The accuracy of the relative measurements is 5% and the accuracy of the absolute calibration is 10% in channel 1 and 20% in channel 3. The full curves show a model phase function form Phobos (Lumme, 1986), matched with the experimental data (light circles) by the method of least squares. The values of the fitting parameters are p = 0.070 ± 0.008 and Γ = 0.046 ± 0.035 (visible) and p = 0.061 ± 0.013 and Γ = 0.325 ± 0.89 (near IR).

© American Institute of Physics • Provided by the NASA Astrophysics Data System

1990SvAL...16..160A

graphs in the near IR. In Fig. 4 we show the brightness factor (ρ), averaged over the disk of Phobos, as a function of phase angle (α) in channels 1 and 3 of the VSC. Here we used ground-based calibration of the absolute sensitivity of the VSC, corrected to allow for the decrease in the sensitivity of the CCD array with decreasing temperature. In the analysis we allowed for the variation of the projected area of Phobos on the plane of the sky, for which we used the model of a triaxial ellipsoid (Duxbury, 1989). An additional scale-factor correction was made so that the area of the illuminated part of the projection of the ellipsoid best matched the visible area of Phobos on the VSC images. To approximate the experimental data, we used a model (Lumme, 1986) of the integrated phase function of Phobos, the parameters of which are the geometrical albedo p and the parameter Γ, which determines the shape of the phase function. The geometrical albedo in the visible, $p = 0.070 \pm 0.008$, and the phase function agree well with previous results (Lumme, 1986). In the near IR, in which the brightness of Phobos had not been measured before, the geometrical albedo, $p = 0.061 \pm 0.013$, does not differ from the value in the visible by more than the measurement errors, but the phase function is somewhat steeper, and this difference is statistically significant (at the 95% confidence level).

An important auxiliary task of the TV photography of Phobos from Mars orbit was to refine the orbital motion of Phobos to correct the course of the AIS as it approached Phobos. These navigational measurements made it possible to reduce the error in predicting the position of Phobos by an order of magnitude — to several kilometers. The mass of Phobos was also improved: $(1.08 \pm 0.01) \cdot 10^{19}$ g (Kolyuka et al., 1990). Assuming the volume of Phobos to be 5530 ± 300 km^3 (Duxbury, 1989), we obtain 1.95 ± 0.1 g/cm^3 for its mean density, which is lower than the density of practically all types of meteorites (Wasson, 1974). The difference from the density of type I carbonaceous chondrites is small and could be explained by the presence of a thick surface layer of regolith and by fractures in the body of Phobos. Other spectral analogs of the material of Phobos — type C3-C4 carbonaceous chondrites (Bibring et al., 1989) and black chondrites (Britt and Pieters, 1988) — have a considerably higher density and compel us to assume that Phobos has considerably porosity or also contains light components such as ice.

There is much work ahead on processing the information acquired, which will take the following directions: improvement of the figure and topographic and geological maps of the surface of Phobos; investigation of the local and integrated spectral and angular reflective characteristics of the surface of Phobos to estimate the optical parameters of the surface, its composition and texture, and their spatial variations: refinement of the librational motion and the position of the center of mass of Phobos to estimate the degree of its uniformity.

In conclusion, we express our gratitude to all the specialists who took part in the preparation and execution of the television experiment.

Bibring, J.-P., Combes, M., Langevin, Y., et al. (1989). Nature (London) 341, 591.
Britt, D. T., and Pieters, C. M. (1988). Astron. Vestn. 22, 229
Duxbury, T. C. (1989). Icarus 78, 169.
Duxbury, T. C., and Callahan, J. D. (1989). Acarus 77, 275.
Head, J. 1986), in: Scientific and Methodological Aspects of the Phobos Study, Space Research Inst., Moscow, p. 61.
Head, J., and Cintala, M. (1979). in: Reports of the Planetary Geology Program 1978-1979, NASA TM-80339, p. 19.
Kolyuka, Yu. F., Efimov, A. E., Kudryavtsev, S. M., et al. (1990). Pis'ma Astron. Zh. 16, 396 [Sov. Astron. Lett. 16, 168 (1990)].
Lumme, K. (1986). in: Scientific and Methodological Aspects of the Phobos Study, Space Research Inst., Moscow, p. 97.
Noland, M., and Veverka, J. (1976). Icarus 28, 404.
Pang, K. D., Rhoads, J. W., Hanover, G. A., et al. (1983). J. Geophys. Res. 88, 2475.
Shkuratov, Yu. G. (1988). Kinemat. Fiz. Nebesn. Tel 4, 33.
Thomas, P. (1978). Rep. 693, Center for Radiophysics and Space Research, Cornell Univ., Ithaca, N.Y.
Thomas, P. (1979). Icarus 40, 223.
Thomas, P., Veverka, J., Bloom, A., and Duxbury, T. (1979). J. Geophys. Res. 84, 8457.
Turner, R. J. (1978). Icarus 33, 116.
Veverka, J. (1978). Vistas Astron. 22, 163.
Wasson, J. (1974). Meteorites, Springer-Verlag, New York.
Wilson, L., and Head, J. (1989). Lunar Planet. Sci. 20, 1211.
Zellner, B. N., and Capen, R. C. (1974). Icarus 23, 437.

Translated by Edward U. Oldham

© American Institute of Physics • Provided by the NASA Astrophysics Data System